

# Droplet actuation and droplet mobility manipulation on porous surfaces by means of backpressure control

N. Vourdas and V.N. Stathopoulos

School of Technological Applications, Technological Educational Institute of Sterea Ellada, Psahna, 34400, Evia, Greece, nvourdas@teihal.gr, vasta@teihal.gr

## ABSTRACT

We present our work on the droplet actuation and mobility manipulation on hydrophobic porous medium. We use a porous medium under which the pressure is controlled (backpressure), thus ensuring a constant gas flow under the droplet. Different modes of droplet actuation are identified, depending on the droplet volume. For large droplets, movement is recorded upon bubble rupturing, while for smaller droplets a gas cushion is formed after a critical pressure value. The sliding angle of droplets with various volumes was measured for a range of backpressure values. The sliding angle, e.g. for a 50  $\mu\text{l}$  droplet decreases from  $22^\circ$  to  $0^\circ$  when the backpressure increases to 0.800 bar. Application is demonstrated on a fluidic, thus providing an alternative means for valving.

**Keywords:** wetting transitions, droplet mobility, droplet actuation, porous membranes, valving

## 1 INTRODUCTION

Control over the mobility of droplets on surfaces remains an important part of recent research activity, both for understanding the pertaining wetting principles [1] as well as for practical applications including microfluidics [2, 3] and chemical processes in droplets [4], engineered self-cleaning surfaces [5-7], membrane contactors [8], polymer electrolyte fuel cells [9] etc.

In this direction approaches towards manipulating the mobility of a droplet, based on the respective wetting transitions, are far from rare. Pertinent methodologies have been reviewed at Refs [10-13].

In most cases the mobility of a droplet, and the gradual conversion from a pinned to a slippery state is assessed by measuring the so called sliding angle, i.e. the minimum angle which a surface has to be tilted in order to inseminate moving of the droplet, by sliding or rolling. Many studies have been reported towards understanding the mechanisms during droplet movement; sliding or rolling [14-16]. Of particular importance is the trailing edge of the droplet at which the contact angle ( $\theta_r$ ) is much lower than the contact

angle at the leading face ( $\theta_a$ ). Paxson et al [17] followed the detachment of water droplet at the trailing edge, from textured surfaces using environmental scanning electron microscopy and developed a model to predict the adhesion force and proposed rules to design surfaces with low adhesion. The case of a complex interface (oil-air-water and oil-water-solid) has been treated by Smith et al [18] who introduced an effective pinning force due to the existence of the additional contact line, applicable for the lubricant-impregnated surfaces.

Recently our group has presented a method to control the mobility of a water droplet after impingement on porous medium [19]. The pressure at the rear phase of the porous medium (backpressure) is deliberately tuned, to adjust the pressure balance at the front phase of the medium. Overpressure at the rear phase favors the antiwetting factor and results in a slippery droplet, whereas underpressure results in sticky droplet.

Even though the case of drops levitated by an air cushion by a air stream flowing under a droplet is not new and has been given extensive theoretical focus [12, 20-23], yet its application towards droplet actuation and mobility manipulation has been treated very recently [19, 24]. Extensive analysis has been performed for the case of one gas bubble that has been introduced by means of a pipette on the effect of mobility on a inclined surface [25-28]

In this work we present our study on the droplet actuation and droplet mobility manipulation by means of pneumatic scheme and using a porous medium. The porous hydrophobic medium acts as gas supply distributor, in order to provide continuous gas flow under the droplet. Deliberate backpressure control leverage respective mobility droplet wetting transitions, from sticky to slippery state.

## 2 EXPERIMENTAL

Porous media (membranes) were fabricated from  $\alpha\text{-Al}_2\text{O}_3$  powder, with a particle size distribution, in

which the 90% of the particles had diameter less than 7.0  $\mu\text{m}$  i.e.  $D_{0.9}=7.0 \mu\text{m}$ .  $(\text{NH}_4)_2\text{HPO}_4$  was added to  $\text{Al}_2\text{O}_3$  powder as much as 5%wt and the mixture was uniaxially pressed under 110 MPa to form green disk shaped membranes with diameter of 13 mm. A similar procedure was followed to form membranes with diameter of 32 mm. The final membranes were prepared after sintering the green samples for 3 h at 1000 °C. At this stage, the membranes are superhydrophilic and water absorbing.

To render the initially superhydrophilic and water absorbing surface into a hydrophobic one, all the membranes were infiltrated with 0.5%wt Teflon solution (poly(4,5-difluoro-2,2-bis(trifluoromethyl)-1,3-dioxole-co-tetrafluoroethylene in Fluorinert FC-770) and then heated up to 110 °C for 20 min. This approach was employed as one of the most facile methods to coat the membranes with Teflon. Experiments have been also performed on membranes deposited via vapor deposition with appropriate precursor. The final thickness of the membranes was at maximum  $h=2 \text{ mm}$  to provide adequate mechanical strength upon backpressure application. The selection of this powder was to minimize the pressure drop along the membrane [19].

Scanning Electron Microscopy (SEM) image of the  $D_{0.9}=7.0 \mu\text{m}$  hydrophobic membrane, i.e. after Teflon coating, is presented in Figure 1.

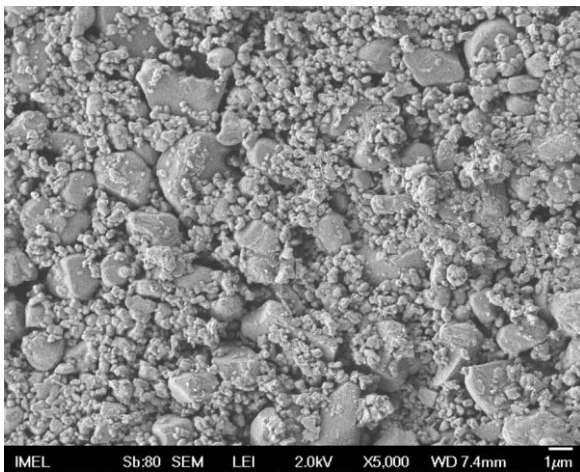


Figure 1. SEM image of the hydrophobic porous medium used in this study ( $\alpha\text{-Al}_2\text{O}_3$ ,  $D_{0.9}=7.0 \mu\text{m}$ ).

The hydrophobic porous medium was positioned on a perforated plexiglas sheet under which the gas pressure is controlled using needle valve and a manometer with accuracy of  $\pm 2 \text{ mbar}$ . In all cases presented herein air was used as the pneumatic means for actuation and mobility manipulation.

### 3 RESULTS AND DISCUSSION

Two modes of droplet transfer have been identified, depending on the droplet volume.

In Figure 2 we present a sequence of snapshots illustrating the transfer mechanism of a large, namely 60  $\mu\text{l}$ , water droplet, during continuous gas flow application at the rear face of the porous, at which the pressure is maintained at 0.800 bar.

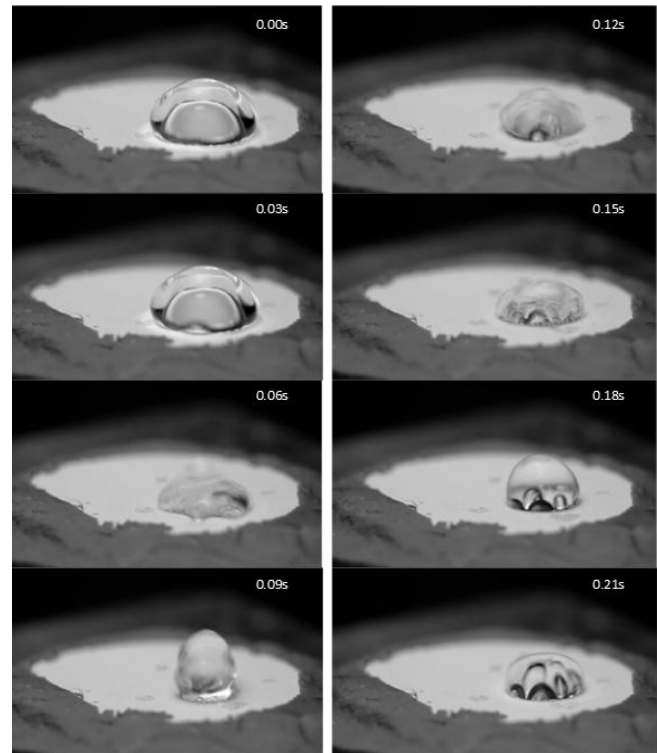


Figure 2. Snapshots of a 60  $\mu\text{l}$  water droplet during actuation. A large bubble has been formed (0.00 s), which gradually deforms the droplet (0.03 s). The bubble ruptures (0.06 s) triggering a depinning (0.09 s). At this point the droplet exhibits high mobility and can be easily moved, e.g. by the presence of a small incline. Up to 0.15 s multiple smaller volume encapsulated bubbles are seen. After that these bubbles are gradually merged to form another large bubble (0.21 s) and trigger another downward movement.

Various small bubbles are progressively merged together to form a large encapsulated bubble, which gradually deform the droplet. At some point the bubble ruptures, thus providing sufficient energy for depinning. The droplet exhibits high mobility, and may move easily, by e.g. the presence of small incline. In Figure 2 the porous medium is only slightly tilted, yet this enables the droplet to move downwards. After this sequence small bubbles appear again at the liquid/solid interface that progressively merge together, thus triggering another movement.

The mechanism is different for the case of smaller droplets. The bubble is not ruptured as in the case of the larger droplets. After a certain pressure value a gas cushion is formed, and if the gas flow is high enough the droplet is kept virtually afloat. Similar phenomena have been studied and analyzed previously [29]. The droplet at this stage exhibits high mobility and may be moved even at the slightest incline. In Figure 3 we present snapshots of a droplet with smaller volume, i.e. 20  $\mu\text{l}$ , compared to the one in Figure 2. The backpressure has been tuned to 1.200 bar.

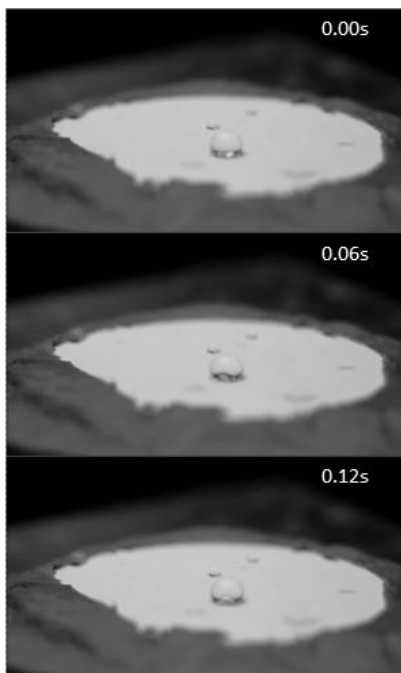


Figure 3. Snapshots of a 20  $\mu\text{l}$  water droplet during actuation. An air cushion has been formed, keeping the droplet virtually afloat. The droplet exhibit high mobility and may be moved even at low values of tilting.

In all cases, both for large and small droplets the mobility switching is reversible, i.e. upon backpressure relief, the droplet pins to the surface. Again after backpressure application the droplet is again actuated as described before. Therefore reversible switching between the sticky and slippery state may be realized.

In Figure 4 the sliding angle of water droplets of various volumes are depicted vs. the applied backpressure. In this work the sliding angle is defined as the minimum angle at which the droplet moves systematically downwards, at some point during backpressure application. In all cases the sliding angle decreases when the backpressure increases, as expected.

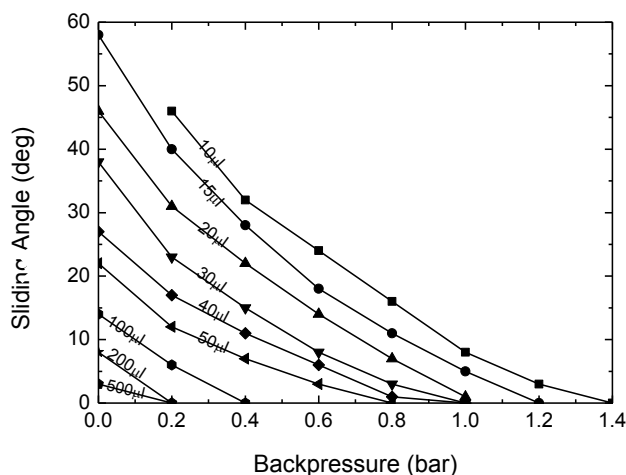


Figure 4. Sliding angle variation of various volume water droplet vs. backpressure (wide survey).

For example the sliding angle of a 20  $\mu\text{l}$  water droplet is ca.  $45^\circ$ , when no backpressure is applied and gradually drops to  $23^\circ$  and  $8^\circ$  when the backpressure increases to 0.400 and 0.800 bar respectively. When the backpressure increases to 2 bar the 20  $\mu\text{l}$  water droplet remains virtually afloat and eventually slides continuously outside the membrane peripheral, as discussed earlier. For smaller backpressure values, at which the air cushion is not fully developed, the movement is not continuous. The 10  $\mu\text{l}$  droplet remains pinned at backpressures lower than 0.200 bar.

The dependence of the sliding angle on droplet volume and backpressure will be followed by using a modified force balance that will encounter the existence of an additional contact line [18], i.e. the one formed because of the encapsulated bubble.

The photos in Figure 5 demonstrate the implementation of our method for liquid mobility control, inside a hydrophobic trench, towards microfluidic applications.



Figure 5. Demonstration of the concept for microfluidic applications (actuation and valving): (i) Initially the water plug inside the fluidic hydrophobic channel is stationary, i.e. the valve is in “closed” mode. (ii) Upon backpressure application, air pockets appear in the solid-water interface and finally (iii) the plug flows through, setting the valve in the “open” mode.

The water plug inside the fluidic is initially sticky. Upon overpressure application under the membrane, the water-solid surface area decreases (see the air pockets formation), the mobility of the plug increases and finally the plug flows through the trench, thus proposing an alternative method for microfluidics actuation and valving [30], without heat dissipation, or usage of electric or magnetic source.

## 4 CONCLUSIONS

We presented a method to actuate and manipulate the mobility of droplets on a hydrophobic porous medium, by means of backpressure control. Two modes of actuation have been identified depending on the droplet volume. For large droplets movement is recorded during bubble rupturing, while for smaller droplets a gas cushion is formed after a certain gas flow value, thus enabling the droplet movement even at low tilt angles. The actuation scheme is reversible, i.e. by adjusting the backpressure the droplet may be pinned to the surface or may be actuated and move, e.g. by the presence of an incline. Sliding angle values have been measured and found to decrease with backpressure and droplet volume. Application of this method for fluidic valving has been demonstrated, providing an alternative means, with no heat dissipation or use of electrical or magnetic sources.

## REFERENCES

- [1] P. G. de Gennes, F. Brochard-Wyart, and D. Quere, *Capillarity and Wetting Phenomena: Drops, Bubbles, Pearls, Waves* (Springer-Verlag, New York, 2004).
- [2] A. C. Glavan *et al.*, *Lab on a chip* **13** (15), 2922 (2013).
- [3] N. Vourdas *et al.*, *Microelectronic Engineering* **85** (5), 1124 (2008).
- [4] H. Song, D. L. Chen, and R. F. Ismagilov, *Angewandte Chemie* **45** (44), 7336 (2006).
- [5] N. Vourdas, A. Tserepi, and E. Gogolides, *Nanotechnology* **18** (12), 125304 (2007).
- [6] N. E. Vourdas *et al.*, *International Journal of Nanotechnology* **6** (1-2), 196 (2009).
- [7] K. Tsougeni *et al.*, *Langmuir* **25** (19), 11748 (2009).
- [8] S. Mosadegh-Sedghi *et al.*, *Journal of Membrane Science* **452** (0), 332 (2014).
- [9] F. Y. Zhang, X. G. Yang, and C. Y. Wang, *Journal of the Electrochemical Society* **153** (2), A225 (2006).
- [10] E. Bormashenko, *Advances in colloid and interface science*, in press (2014).
- [11] G. Whyman, and E. Bormashenko, *Journal of Adhesion Science and Technology* **26**, 207 (2012).
- [12] M. Reyssat *et al.*, *Faraday Discussions* **146** (0), 19 (2010).
- [13] N. Verplanck *et al.*, *Nanoscale Research Letters* **2** (12), 577 (2007).
- [14] E. Pierce, F. J. Carmona, and A. Amirfazli, *Colloids and Surfaces A: Physicochemical and Engineering Aspects* **323** (1-3), 73 (2008).
- [15] M. K. Chaudhury, and P. S. Goohpattader, *The European physical journal. E, Soft matter* **36** (2), 15 (2013).
- [16] B. Krasovitski, and A. Marmur, *Langmuir* **21**, 3881 (2005).
- [17] A. T. Paxson, and K. K. Varanasi, *Nature communications* **4**, 1492 (2013).
- [18] J. D. Smith *et al.*, *Soft Matter* **9** (6), 1772 (2013).
- [19] N. Vourdas, A. Tserepi, and V. N. Stathopoulos, *Applied Physics Letters* **103** (11), 111602 (2013).
- [20] M. A. Goldshtik, V. M. Khanin, and V. G. Ligai, *Journal of Fluid Mechanics* **166**, 1 (1986).
- [21] P. Brunet, and J. H. Snoeijer, *The European Physical Journal Special Topics* **192** (1), 207 (2011).
- [22] W. Bouwhuis *et al.*, *Physical Review E* **88** (2) (2013).
- [23] M. Papoular, and C. Parayre, *Physical Review Letters* **78** (11), 2120 (1997).
- [24] J. N. Tan, W. Y. L. Ling, and A. Neild, *Applied Physics Express* **6** (7), 077301 (2013).
- [25] C. Antonini *et al.*, *Langmuir* **25** (11), 6143 (2009).
- [26] W. Y. Ling, G. Lu, and T. W. Ng, *Langmuir* **27** (7), 3233 (2011).
- [27] W. Y. Ling, T. W. Ng, and A. Neild, *Langmuir* **26** (22), 17695 (2010).
- [28] W. Y. Liang Ling *et al.*, *J Colloid Interface Sci* **354** (2), 832 (2011).
- [29] J. Snoeijer, P. Brunet, and J. Eggers, *Physical Review E* **79** (3) (2009).
- [30] N. T. Nguyen, presented at the 3rd European Conference on Microfluidics-Microfluidics 2012, Heidelberg, 2012.